R. & M. No. 2962
(16,338)
A.R.C. Technical Report

ROYAL AIRCRAFT ESTABLISHMENT
LIBRARY
BEDFORD.

MINISTRY OF SUPPLY

AERONAUTICAL RESEARCH COUNCIL
REPORTS AND MEMORANDA

Control Surfaces Restrained by Viscous Friction as a Means of Damping Aircraft Oscillations

By

W. J. G. PINSKER

Crown Copyright Reserved

LONDON: HER MAJESTY'S STATIONERY OFFICE
1957
PRICE 7*s* 6*d* NET

Control Surfaces Restrained by Viscous Friction as a Means of Damping Aircraft Oscillations

By

W. J. G. Pinsker

Communicated by the Principal Director of Scientific Research (Air),
Ministry of Supply

Reports and Memoranda No. 2962*

February, 1953

Summary.—A method is described of controlling the phase of the free motion of control surfaces by viscous friction and geared masses. Substantial improvements in the damping of aircraft oscillations can be achieved if such devices are applied to existing or additional control surfaces or to tabs attached to such controls. The merits of various arrangements are discussed and formulae for the determination of optimum conditions are derived.

The conclusions are illustrated by numerical examples.

1. *Introduction*.—The dynamic stability and in particular the lateral stability of aircraft tends to deteriorate with the advance of design and performance. There is only very limited scope for improvements in the geometry and inertial loading of the aircraft and even such improvements might easily be offset by later additions to the loading of the aircraft or by other factors unknown in the design stage.

Artificial stabilisation is often the only answer to these difficulties and has been successfully applied in a number of cases[1,2]. With such a system a servomechanism is used to control the rudder so as to oppose the rate of yaw of the aircraft motion and a powerful addition to the damping in yaw and thus to the dynamic lateral stability is achieved.

It can be seen from theoretical investigations[3,4], and from flight evidence[1], that for certain combinations of the aerodynamic and inertial characteristics of a rudder with friction within the rudder circuit, the dynamic lateral stability of an aircraft is considerably improved by the free motion of the rudder. Use can be made of this effect if the rudder is specially designed to obtain such characteristics, and in this report the operational principles and the optimum conditions for such rudder arrangements will be examined. As a result various control arrangements will be described and compared as to their relative merits and limitations. The discussion in the main body of the report will be on a physical basis, the theoretical analysis being confined to appendices. The potentialities of the various proposals will be illustrated by numerical examples.

During the preparation of this paper, flight tests with a *Vampire* Mk. 5, with one rudder modified to serve as a damping rudder, have been successfully completed.

*R.A.E. Report Aero. 2486, received 24th November, 1953.

In the present report only lateral stability will be considered. Analogous application to horizontal control surfaces can be expected to produce equivalent improvements in dynamic longitudinal stability.

2. *The Damping Rudder.*—2.1. *Operational Principle.*—The following investigations will consider one degree of freedom (in yaw, ψ) of the aircraft motion only. This restriction will greatly simplify the discussion and will hardly affect the validity of the conclusions. It can be proved that with all conceivable practical aircraft configurations the action of the rudder will hardly alter the motion of the aircraft in the two neglected freedoms : rolling and sideways movement of the c.g. On the other hand these freedoms will generally alter the relationship between yawing and sideslipping so as to make $(-\beta) \geqslant \psi$. This implies that the main results obtained from the following analysis, namely the Δn_r derivatives—which can be proved to be proportional to $-\beta/\psi$—will be generally smaller than those corresponding to the unrestricted aircraft motion and will thus generally be a conservative estimate.

If a rudder, underbalanced in $b_1 (b_1 < 0)$, is freely hinged to the fin of an aircraft it will tend to align itself with the local flow. During directional oscillations of the aircraft the rudder will then move in counterphase to the aircraft as sketched below for three successive stages of an oscillation, the intervals being $\frac{1}{4}$ periods.

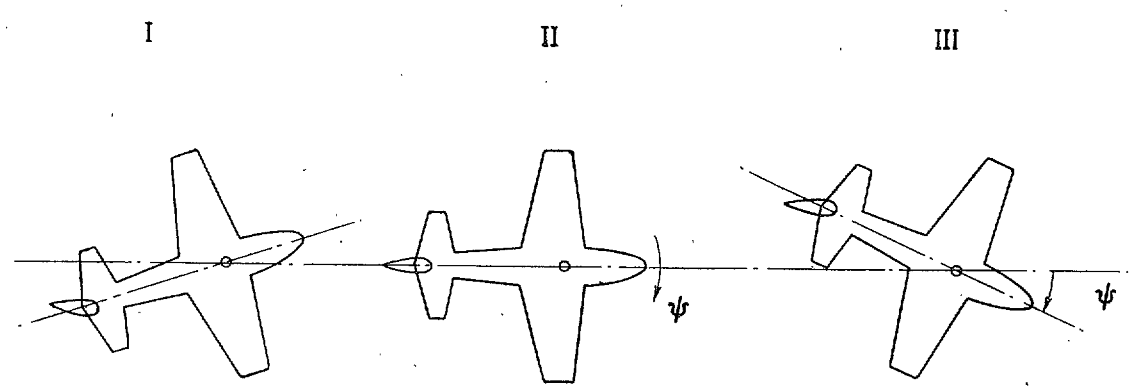

At instant II the aircraft swings through its centre position at maximum rate of yaw $\dot{\psi}$. If one neglects the small flow contribution due to rotation no rudder deflection occurs at this instant and consequently the damping of the aircraft is not affected. The rudder, ζ, however, floating in counterphase to the aircraft deflection ψ reduces the effective weathercock stability and thus the frequency of the aircraft oscillation. The rudder exerts upon the aircraft a yawing moment

$$\Delta C_N = n_\zeta \zeta \qquad \qquad (1)$$

ζ being in phase with $(-\psi) = \beta$. This represents an additional n_v derivative :

$$\Delta n_v = \frac{\partial \Delta C_N}{\partial \beta} = -\frac{\zeta}{\psi} n_\zeta .$$

If rudder mass and inertia are neglected the rudder floating is given by the quasi-steady relationship $\zeta/\psi = -b_1/b_2$ and

$$\Delta n_v = +\frac{b_1}{b_2} n_\zeta . \qquad \qquad (2)$$

If the motion of the rudder were delayed by $\frac{1}{4}$ period, as illustrated below, the rudder would deflect in the rate of turn phase (stage II) of the aircraft motion in a sense as to oppose it and thus to damp it.

I II III

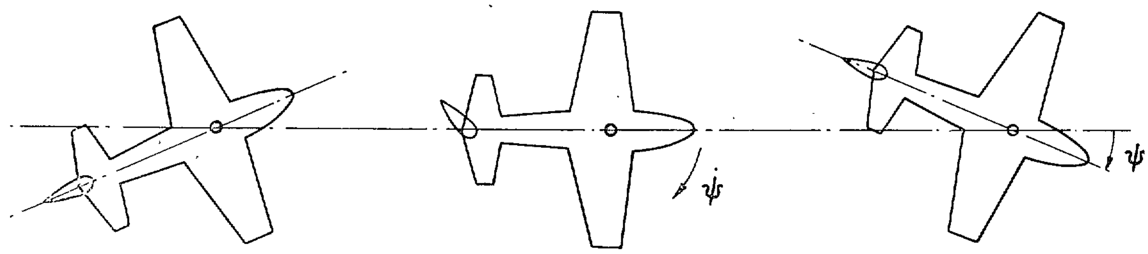

Its yawing moment, equation (1), can now be expressed as a damping in yaw derivative

$$\Delta n_r = \frac{\partial \Delta C_N}{\partial \frac{rb}{2V}} = \frac{\zeta}{\dot\psi}\frac{2V}{b} n_\zeta .$$

Since the rate of yaw amplitude $\dot\psi = \psi\omega = \psi 2\pi / T_\psi$ (correct only for undamped oscillations) this gives :

$$\Delta n_r = \left| \frac{\zeta}{\psi} \right| \frac{T_\psi}{2\pi} \frac{2V}{b} n_\zeta . \qquad (3)$$

If the rudder amplitude ζ is the same as for the case without phase lag this gives finally

$$\Delta n_r = + \frac{b_1}{b_2} \frac{T_\psi V}{2\pi} \frac{2}{b} n_\zeta \qquad (4)$$

Δn_r will be negative, *i.e.*, damping, if b_1/b_2 is positive (rudder aerodynamically underbalanced). This represents the ideal rudder response with respect to aircraft damping.

Phase lag of the rudder response can be affected by viscous or solid friction. Solid friction would be ruled out for practical applications, since it will jam the control at small amplitude oscillations and make the rudder inefficient for aircraft damping in that range when improvements are often wanted most. As explained in Appendix B the phase lag obtainable by friction is limited practically to the range of 0 to 90 deg, the optimum aircraft damping being obtained with about 45 deg, *i.e.*, $\frac{1}{8}$ of a period. In this case the rudder will both reduce the frequency and contribute to the damping of the directional oscillation as illustrated below.

I II III

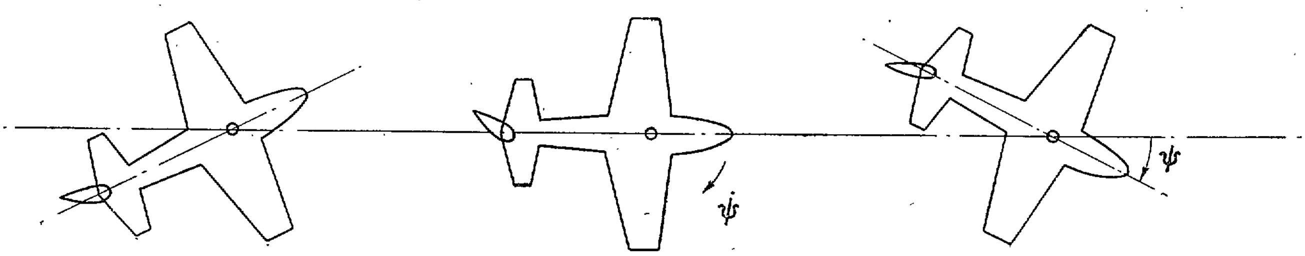

Quantitatively the contribution of the rudder to n_v and n_r depends on the actual relative rudder amplitude ζ/ψ and the phase angle ε_ζ of its motion. As distinct from the assumptions in equation (4) the rudder amplitude will generally be reduced by the effect of the phase-shifting device. In order to assess Δn_v and Δn_r the rudder yawing moment ΔC_N has to be split up into its two components in phase with ψ and with $\dot{\psi}$. If ε_ζ is the phase angle between ζ and ψ, positive ε_ζ corresponding to phase advance of the rudder, this gives :

$$\Delta n_v = -\frac{\zeta}{\psi} n_\zeta \cos \varepsilon_\zeta \qquad \ldots \qquad (5)$$

$$\Delta n_r = \frac{\zeta}{\psi} \frac{T_\psi V}{2\pi} \frac{2}{b} n_\zeta \sin \varepsilon_\psi \, . \qquad \ldots \qquad (6)$$

A more detailed analysis considering also the effect of rudder inertia and mass moment is given in Appendices A and B.

Analysis so far has shown that a rudder must meet the following requirements if it is to act as an effective yaw-damper.

(i) It must be mechanically free to respond to the motion of the aircraft.

(ii) Its effectiveness increases with the amount of aerodynamic underbalance, *i.e.*, with b_1/b_2.

(iii) The rudder must be retrained by an appropriately dimensioned mechanical damper so as to have its response delayed by roughly $\frac{1}{8}$ of a period of the aircraft oscillation.

These principles must of course be balanced against pilot control requirements. This leads to a number of different arrangements, the relative merits and limitations of which will be discussed below.

2.2. *Damped Main Rudder.*—To act as a yaw-damper the rudder has to be connected to a mechanical damper (dashpot) which restrains its motion as indicated in Fig. 1. The pilot has to operate against the resistance of this dashpot when applying the control. On the other hand the required damping motion of the control is suppressed if the pilot fixes the control. In practice, however, he will not hold the pedals rigidly and, in addition, the elasticity of the control circuit will leave an appreciable amount of rudder freedom. The resistance of the damper in the control circuit will restrict the method to cases where the required stiffness of the damper is reasonably small. In particular, this will be so if the basic pedal forces are moderate. Full benefit is restricted to control free flight and the effectiveness during constantly controlled operations such as aiming may be reduced.

An alternative system which does not suffer from these particular limitations is to arrange the damper within the control circuit as illustrated in Fig. 2. The damper has in this case to be centred by a spring in order to maintain proper co-ordination of the control. With this arrangement, however, no aircraft damping is obtained with the control free, unless there is excessive friction or mass in the control circuit between the damper and the pilot. Pilot's control is affected in so far as the damper gives way to pedal forces until there is equilibrium between the control force and the spring force. With pedals fixed the spring increases the effective rudder b_2 which in turn is detrimental to the effectiveness of the rudder as a yaw damper.

Now, to obtain the effect of either type of damping rudder, reference is made to the results of section 2.1 and to the more extended treatment in Appendix B, where the influence of rudder mass moment and inertia is also considered. If a hydraulic dashpot is used, it will generally be adjusted to give optimum rudder response for a speed, V_{SET}, within the operational range of the aircraft. For this case Appendix B gives :

$$\Delta n_r = n_\zeta \frac{b_1}{b_2}\sqrt{\left(\frac{\rho_0}{\rho}\right)}\frac{T_\psi V_i}{\pi b}\frac{1+\dfrac{\sigma_M-\sigma_\theta}{b_1}}{1+\dfrac{\sigma_\theta}{b_2}}\frac{V_{SET}/V_i}{1+(V_{SET}/V_i)^2}\cdot \qquad \ldots \qquad (7)$$

σ_M and σ_θ represent the effects of rudder mass moment ($m_R x_R$), and rudder inertia, θ, respectively:

$$\sigma_M = 2\frac{m_R l_F x_R}{\left(\dfrac{T_\psi V_i}{2\pi}\right)^2 \rho_0 S_R c_R} \qquad \ldots \qquad (8)$$

$$\sigma_\theta = 2\frac{m_R c_R i_R}{\left(\dfrac{T_\psi V_i}{2\pi}\right)^2 \rho_0 S_R}\cdot \qquad \ldots \qquad (9)$$

Mass overbalance ($x_R < 0$) is beneficial and can be utilised within economical limits. Rudder inertia too is beneficial for Δn_r with $b_2 < b_1$. For $b_2 > b_1$, which will normally be the case, it is detrimental.

If the damping afforded by the rudder-damper is made to vary in proportion to V_i (*see* section 4) the last term in equation (7) will become constant $= \frac{1}{2}$. With a simple hydraulic damper, however, Δn_r is reduced above and below V_{SET} according to the last term in equation (7) as plotted in Fig. 3.

Throughout this analysis the natural frequency of the lateral oscillation of the aircraft is expressed by the parameter $T_\psi V_i$, i.e., the indicated wave-length. This parameter can generally be assumed to be fairly constant over the operational range of the aircraft.

The required rudder damping for optimum operation is also determined in Appendix B as

$$\frac{\partial H}{\partial \dot{\zeta}} = V_i\left(\frac{T_\psi V_i}{2\pi}\right)\left(1+\frac{\sigma_\theta}{b_2}\right)\frac{\rho_0}{2} b_2 S_R c_R \qquad \ldots \qquad (10)$$

where V_i should be taken as the setting speed, V_{SET}. Also a more accurate graphical method is given for the determination of Δn_v and Δn_r.

2.3. *Damped Additional Rudder.*—The disadvantages of the use of a main control surface as a damping device can be overcome by having separated surfaces for control and damping respectively. The damping surface is disconnected from the control circuit (Fig. 4) ; it can, however, be operated as a pilot's control by means of a servo-tab (Fig. 5). Another method to make the damping rudder available for pilot's control in emergencies is to connect the damping rudder to the control circuit with sufficient backlash to allow the damping rudder to operate as a damper within the limits of the play—say $\pm$ 5 deg. For full pedal operation the damping rudder will follow the main rudder, the pilot having to overcome the resistance of the damper connected to the damping rudder (Fig. 6).

A general arrangement for the installation of a separated damping rudder is sketched in Fig. 7. The bottom part of the rudder is connected to the control circuit in the usual way, has aerodynamic balance and carries the trim tab. The top rudder is restricted by a hydraulic dashpot and has no connection to the control circuit. It is not aerodynamically balanced in order to maintain large negative b_1. It carries a tab as illustrated in Fig. 5 as a servo-control which is also geared to balance b_2.

Equations (7) to (10) apply for this type of damping rudder as well if the geometrical, inertial, and aerodynamic parameters used are those of the damping rudder only.

3. *Damping Tab.*—3.1. *Operational Principle.*—If a tab is freely hinged to a rudder which for simplicity of analysis is assumed to be aerodynamically and inertially neutral, the response of the rudder to the lateral oscillation of the aircraft will then be entirely determined by the response of the tab itself. Of course an actual rudder will generally have $b_1 \neq 0$ plus inertia, mass moment and friction. All these parameters will make contributions of their own to the rudder response and will also affect the response of the rudder to the tab motion. These effects are considered in Appendix C. For the demonstration of the basic principle, however, the simple case with idealized rudder will suffice.

The aim of the damping tab must be to cause a rudder motion equivalent to that obtained with a 'damping rudder' as described in section 2, *i.e.*, the floating characteristic of the tab must be opposite to that of the 'damping rudder.' Thus the tab must be aerodynamically overbalanced ($c_1 > 0$) and mechanically damped to obtain the required phase delay of ~ 45 deg. With the rudder free the response of such a system to the directional oscillation of the aircraft will be as sketched below :

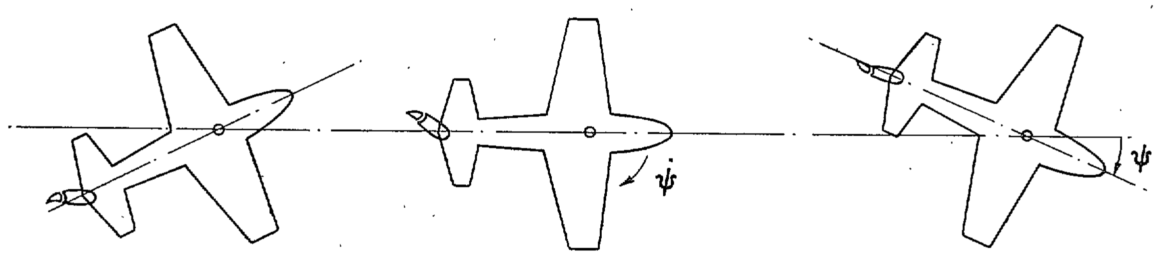

The effect of the tab on the motion of the aircraft is determined by the contribution of the rudder yawing moment on n_v and n_r as given in equation (5) and (6). In the idealized case under discussion the rudder response is basically determined by the quasi-steady relation

$$\frac{\zeta}{\beta} = -\frac{b_3 c_1}{b_2 c_3} \qquad (11)$$

which will be reduced by mechanically damping the tab movement. Instead of, or in addition to, the use of positive c_1, tab mass underbalance can be used to effect an equivalent response. The mass of the tab exerts upon the tab hinge a moment

$$H_T = m_T x_T l_F \ddot{\psi} \, . \qquad (12)$$

For oscillatory motion

$$\ddot{\psi} = -\psi \left(\frac{2\pi}{T_\psi}\right)^2 \simeq \beta \left(\frac{2\pi}{T_\psi}\right)^2 .$$

With this relation equation (12) can be expressed as an apparent c_1 derivative

$$\Delta c_1 = -\frac{C_{HT}}{\partial \beta} = -2 \frac{m_T}{\rho_0} \frac{x_T}{c_T} \frac{l_F}{S_T} \left(\frac{2\pi}{T_\psi V_i}\right)^2 \qquad (13)$$

and substituted into equation (11).

3.2. *Design Considerations.*—The most promising arrangement for a damping tab attached to a rudder is shown in Fig. 8. The pilot has unrestricted rudder control. If the pedals were fixed rigidly, the rudder would be prevented from responding to the tab movement and no aircraft damping would be affected. In practice, however, pilots will not restrain the controls to such an extent as to interfere seriously with the operation of the damping rudder. This has been demonstrated conclusively with autostabilizer-operated tabs. Of course, friction in the rudder circuit must be small enough to allow the rudder to respond to the tab.

As explained in section 3.1 the operation of the damping tab depends mainly on aerodynamic overbalance in c_1 and mass underbalance. It will be difficult to achieve large positive c_1 without overbalancing c_2 and c_3 at the same time ; thus the emphasis will be on mass underbalance which is severely restricted for flutter reasons unless the tab-damper can be relied upon for flutter damping. These limitations will of course restrict the application of a damping tab but where only moderate improvements are required it may offer a useful solution.

The damping tab cannot be used simultaneously as a trim, servo or balance tab but must be an additional item.

Theoretical analysis in Appendix C yields an expression for the effectiveness of the damping tab when assuming the rudder to be aerodynamically and inertially neutral as :

$$\Delta n_r = -4\frac{n_\zeta}{c_3}\frac{b_3}{b_2}\frac{m_T}{\rho_0}\left(\frac{2\pi}{T_\psi V_i}\right)\sqrt{\left(\frac{\rho_0}{\rho}\right)}\frac{i_T c_T - \frac{x_T}{c_T} l_F}{bS_T}\frac{V_{\text{SET}}/V_i}{1+(V_{\text{SET}}/V_i)^2}$$
$$\frac{1+c_1/\tau_\beta}{1-\frac{b_3}{b_2}\frac{\tau_\zeta + c_2}{c_3} - D_R\left(\frac{V_{\text{SET}}}{V_i} - D_r\right)} \qquad \qquad (14)$$

Tab inertia and mass moment are represented by the parameters

$$\tau_\zeta = 2\frac{m_T}{\rho_0 S_T}\left(\frac{2\pi}{T_\psi V_i}\right)^2\left(i_T c_T - \frac{x_T}{c_T} l_F\right)$$

$$\tau_\zeta = 2\frac{m_T}{\rho_0 S_T}\left(\frac{2\pi}{T_\psi V_i}\right)^2\left\{i_T c_T\left(1-\frac{b_2}{b_3}\right) - \frac{x_T}{c_T} l_T\right\} \qquad \qquad (15)$$

$$\tau_{\theta T} = 2 i_T c_T \frac{m_T}{\rho_0 S_T}\left(\frac{2\pi}{T_\psi V_i}\right)^2 .$$

τ_β and τ_ζ are positive for mass underbalance ($x_T < 0$). D_R represents rudder damping due to friction within the control circuit and is defined as :

$$D_R = \left(\frac{\partial H}{\partial \xi}\right)\left(\frac{2\pi}{T_\psi V_i}\right)\frac{2}{\rho_0 V_i S_R c_R b_2} \qquad \qquad (16)$$

With moderate friction D_R can be neglected. The tab damping required for optimum effectiveness is obtained in Appendix C as

$$\frac{\partial H_T}{\partial \xi_T} = V_i \frac{\rho_0}{2} S_T c_T\left(\frac{T_\psi V_i}{2\pi}\right)\frac{1-\frac{b_3}{b_2}\left(\frac{\tau_\zeta + c_2}{c_3}\right) - D_R\left(1+\frac{\tau_{\theta T}}{c_3}\right)}{1-D_R} \qquad \qquad (17)$$

It can be seen from equation (14) that the Δn_r obtained from a damping tab increases in proportion with tab and rudder effectiveness, n_ξ and b_3, and that it is inversely proportional to the restoring derivatives b_2 and c_3. Negative c_2 is beneficial but the effect of tab inertia, depends upon the co-ordination of the aerodynamic tab parameters.

More general treatment of a system with rudder b_1, inertia and mass moment makes the results too involved for practical purposes. A simple criterion can, however, be obtained in order to determine whether or not the rudder characteristics are aiding the effect of the damping tab for aircraft damping. It has been shown elsewhere (Refs. 3, 4) and it can indeed be deduced from section 2, that basically the motion of the free rudder with friction damps the motion of the aircraft if $b_1 < 0$ and *vice versa*. This tendency will be reduced if

$$c_2 \leqslant 2\frac{m_T}{\rho_0}\left(\frac{2\pi}{T_\psi V_i}\right)\frac{x_T}{c_T}\frac{l_T}{S_T}\left(1 + i_T\frac{c_T{}^2}{x_T l_T}\right). \qquad (18)$$

This equation determines whether the reaction of the tab to rudder motion—other than that induced by the tab itself—is dominated by c_2 or by the tab mass. In the first case the tab acts effectively as a balance tab for b_2, thus assisting the rudder floating characteristic. If the tab mass moment dominates the tab will respond to rudder deflections in the opposite sense and thus restrain the basic rudder floating.

4. *Design Considerations for Dampers.*—4.1. *Hydraulic Dampers.*—The main feature common to all proposed arrangements is a damper restraining the motion of the control surface concerned. Experience with fluid dampers has shown the following main problems :

(i) The damping required for optimum operation (equations (10), (17)) varies in proportion to V_i, to the wavelength of the aircraft oscillation (TV_i), and with b_2 or c_3 respectively. Optimum operational conditions could be maintained over the speed range of the aircraft by applying a suitably controlled by-pass to the design (Fig. 9).

(ii) Compensation for the viscosity changes of mineral damping fluids is not practicable for the range of temperatures met in flight. Thermostatic heating is unavoidable if such fluids are to be used satisfactorily. Synthetic damping fluids (Silicone) as used for the tests on a *Vampire* have substantially smaller temperature-viscosity coefficients. These are within the scope of conventional temperature compensation devices, which consist usually of a bypass through the piston of the dashpot which is controlled by a mechanism utilising bimetallic expansion.

4.2. *Aerodynamic Dampers.*—The ideally required variation in damping with V_i as mentioned under (i) is obtained by the use of a set of paddles rotating in the airstream and geared to the hinge axis of the control concerned. The damping provided by such an aerodynamic damper (Fig. 10) is

$$h_{\dot\xi} = \frac{\partial C_H}{\partial \dfrac{\dot\xi c_R}{V}} = -\left(G\frac{l_B}{c_R}\right)^2 \frac{S_B}{S_R}(a_i)_B \qquad (19)$$

where

$$\left.\begin{array}{ll} G & \text{gearing} \\ l_B & \text{arm} \\ S_B & \text{total area} \\ (a_i)_B & \text{lift slope} \end{array}\right\} \text{of the rotating blades.}$$

Substituting for h_ξ in equation (10), the required gearing for a given set of paddles is obtained as

$$G^2 = \frac{S_R}{S_B}\frac{b_2}{(a_i)_B}\frac{c_R}{l_B^2}\left(\frac{T_\psi V_i}{2\pi}\right)\left(1+\frac{\sigma_\theta}{b_2}\right)\sqrt{\left(\frac{\rho_0}{\rho}\right)}. \quad \ldots \quad \ldots \quad \ldots \quad \ldots \qquad (20)$$

The blades of such a damper must be correctly trimmed and not subject to icing, otherwise they will move the rudder out of trim ; these requirements may actually be difficult to meet in a service aircraft.

5. *Numerical Examples.*—The actual possibilities of the various damping devices will best be illustrated by numerical examples. To cover the main application four configurations are considered :

Aircraft A	Small personal aircraft, main rudder damped.
Aircraft B	Twin-fin fighter (*Vampire* type) with one of its two rudders used as damping rudder only. Trailing-edge cords for large b_1/b_2 and small mass overbalance.
Aircraft C	Two-engined fighter (*Meteor* type) with part of the total rudder area separated and controlled by a servo-tab only which is also geared as a balance tab.
Aircraft D	Same aircraft as example C but normal rudder control with an additional damping tab hinged to the rudder.

Details of the assumed dimensions and aerodynamic data for the four versions are given in Table 2. The increase in aircraft damping Δn_r has been calculated from equation (10) and (13) assuming the rudder—or tab-damper respectively to be set for a fixed speed which has been chosen as $V_{\mathrm{SET}} = 80$ m.p.h. for example A and 400 m.p.h. for the three fighter versions B—C—D. The results are given in Figs. 11 to 14 covering the range of operational altitudes 0 to 10,000 ft and 0 to 40,000 ft respectively. It is seen that Δn_r increases with height as $\sqrt{(\rho_0/\rho)}$ (*see* equation (7)). Provided the other parameters involved are not altered the log decrement of the lateral oscillation increases with n_r and height as $\Delta\delta \propto \Delta n_r\sqrt{(\rho/\rho_0)}$. Thus the effects of density on Δn_r and on $\Delta\delta$ cancel each other and the gain in decrement $\Delta\delta$ from the damping rudder should be independent of height and vary with V_i only.

The gain in aircraft damping determined is several times the basic damping of the aircraft in all cases. In some cases (examples C and C) the lateral oscillation of the aircraft can be expected to be almost asymptotically damped. Even if some of the assumptions made in the calculations should prove too optimistic the improvements would still be substantial.

Example A (Fig. 11) shows the smallest improvement in spite of the fact that here the full rudder area is utilised for damping. This is mainly due to the short tail arm and to the relatively short wavelength of the lateral oscillation ($T_\psi V_i$) which is a main factor in equation (7). Still, the overall damping is roughly trebled by the operation of the damper. The required rudder damping (according to equation (10) ($\partial H/\partial_\xi = 0\cdot 41\ 10^{-3}$ lb ft/deg/sec) will hardly be objectionable to the pilot.

The gain with example B (Fig. 12) is of a similar order.

Example C (Fig. 13) shows clearly the beneficial effect of the balance tab (reducing b_2) which nearly trebles the effect of the otherwise similar arrangement in example B.

The damping tab (example D, Fig. 14) produces an improvement of the same order. It is, however, doubtful whether the assumed amount of mass moment can in an actual case be installed without overstepping flutter limitations. But even severe restriction should leave some freedom for improvements.

It is worth noting that the drop in Δn_r above and below V_{SET} associated with fixed damper setting is reduced in the case of the damping tab (shown by the denominator of the last term in equation (14)).

If aerodynamic dampers (*see* section 4) are used the change of Δn_r with speed disappears and the optimum values, corresponding to $V_i = V_{\text{SET}}$ are maintained throughout the speed range.

6. *Conclusions.*—It is shown that the motion of freely hinged control surfaces is capable of effecting powerful aircraft damping, if the phase of the movement of the control is delayed by viscous friction. The three following arrangements have emerged from the analysis as the most practical alternatives :

(i) In which a main control surface of an aircraft has negative b_1 and is restrained in its movement by a damper so that with controls free the surface moves in the desired phase. The disadvantages of this scheme are that the resulting damping effect is reduced if the pilot resists the movement of the control and he has to overcome the resistance of the damper when moving the control.

(ii) In which part of the total control surface is separated from the control circuit and restrained by a damper instead. The lost control power may be restored by means of a servo-tab without imposing restrictions upon the pilot's control.

(iii) An additional tab is hinged to an existing control surface. If this tab is aerodynamically overbalanced in c_1 and/or mass underbalanced, it will respond to the motion of the aircraft in such a way as to cause the main control surface to damp the aircraft motion. Pilot's control is unimpaired but holding the control will again reduce the effectiveness of the system.

Consideration of hydraulic dampers has shown that the maintenance of constant viscosity of the damping medium over the temperature range met in flight is the main problem, requiring either thermostatic heating or the use of synthetic oils (silicones). As an alternative to hydraulic dampers paddles rotating in the free stream and geared to the control surface may be considered.

In a number of examples it has been shown that the damping rudder can give large increases in the aircraft damping in yaw and in favourable cases nearly asymptotic damping may be achieved.

LIST OF SYMBOLS

b		Wing span	
b_1	=	$-\partial C_H/\partial\beta$	rudder hinge-moment derivatives
b_2	=	$\partial C_H/\partial\zeta$	
b_3	=	$\partial C_H/\partial\zeta_T$	
c_R		Rudder mean chord	
c_T		Tab mean chord	
c_1	=	$-\partial C_{HT}/\partial\beta$	tab hinge-moment derivatives
c_2	=	$\partial C_{HT}/\partial\zeta$	
c_3	=	$\partial C_{HT}/\partial\zeta_T$	
H		Rudder hinge moment	
$h_{\dot{\zeta}}$	=	$\partial C_H/\partial(\dot{\zeta}c_R/V)$	
H_T		Tab hinge moment	
i_R	=	$\theta/m_R c_R^2$, Rudder inertia coefficient	
i_T	=	$\theta_T/m_T c_T^2$, Tab inertia coefficient	
l_F		Fin arm with respect to aircraft c.g.	
l_T		Distance tab hinge—rudder hinge	
m_R		Rudder mass	

LIST OF SYMBOLS—*continued*

m_T		Tab mass
n_v		Weathercock stability
Δn_v		Contribution of rudder motion to n_v
n_r		Damping in yaw derivative
Δn_r		Contribution of rudder motion to n_r
n_ζ	=	$\partial C_N/\partial \zeta$, Rudder effectiveness
S_R		Rudder area
S_T		Tab area
T_ψ		Period of lateral oscillation
V		Speed
V_i		Indicated speed
V_{SET}		Speed of optimum damper setting
x_R		Distance rudder c.g.—rudder hinge axis (positive for overbalance)
x_T		Distance tab c.g.—tab hinge axis (positive for overbalance)
β		Angle of sideslip
ε		Phase angle (positive for phase advance)
ε_R		Change in rudder phase due to friction
ε_ζ		Phase of rudder deflection with respect to ψ
ψ		Angle of yaw
σ_M		Rudder mass moment parameter } Equation (8)
σ_θ		Rudder inertia parameter } Equation (9)
τ_β, τ_ζ		Tab mass and inertia parameters } Equations (15)
$\tau_{\theta T}$		Tab inertia parameter } Equations (15)
θ		Rudder inertia
θ_T		Tab inertia
ζ		Rudder deflection } Positive with trailing edge to port
ζ_T		Tab deflection } Positive with trailing edge to port
ω_ψ		Angular frequency of the lateral oscillation

REFERENCES

No.	*Author*	*Title, etc.*
1	K. H. Doetsch	Interim report on snaking behaviour of the *Meteor* III. R.A.E. Report Aero. 2288. A.R.C. 11,947. August, 1948.
2	Roland J. White	Investigations of lateral dynamic stability in the XB–47 airplane. *J. Ae. Sci.* Vol. 17, No. 3. March, 1950.
3	H. Greenberg and L. Sternfield	A theoretical investigation of the lateral oscillation of an aeroplane with rudder free, with special reference to the effect of friction. N.A.C.A. Report 762. March, 1943.
4	S. Neumark	A simplified theory of the lateral oscillation of an aeroplane with rudder free, including the effect of friction in the control system. R. & M. 2259. May, 1945.

TABLE 1

Comparison of the Various Rudder Arrangements Discussed

Effect	System				
	Damped main rudder		Damped separated rudder		Damping tab
	Damper at control	Damper within control circuit	Free damping rudder	Servo-controlled damping rudder	
Static pedal forces	Unchanged	Unchanged	Reduced	Reduced	Unchanged
Dynamic pedal forces	Much increased	Unchanged	Reduced	Reduced	Unchanged
Max. rudder power	Unchanged	Reducing with increased speed	Reduced	Slightly reduced	Unchanged
Aircraft response to control application	Delayed	Slightly delayed	Unchanged	Slightly delayed	Unchanged
Damping effect with pedals free	Good	Little	Good	Very good	Moderate
Damping effect with pedals fixed rigidly	Little	Good	Good	Very good	Little
Effect of loss of viscous friction in damper	Aircraft back to normal	Pedals spongy	Loss of additional damping	Loss of additional damping	Loss of additional damping
Effect of jammed damper	Need for override clutch, otherwise loss of control	Aircraft back to normal	Aircraft back to normal	Reduced control power	Loss of additional damping
Main applications	Small aircraft with low speed	General	Aircraft requiring little rudder power	General	General mainly low-speed aircraft

TABLE 2

Dimensions and Data of the Four Aircraft Considered with the Numerical Examples

Aircraft	A	B	C	D
Number of fins	1	2	1	1
Damping arrangement	Damped main control	Damped separated rudder	Separated rudder with balance tab	Damping tab on main rudder
Weight, W, lb	1,500	10,000	14,000	14,000
Wing area, S, ft² ..	150	250	400	400
Span ft	30	38	40	40
Total fin area, S_F, ft² ..	10	25	35	35
fin arm, l_F, ft ..	14	17	27	27
Damping Rudder				
Area, S_R, ft²	5	4	5	10
Chord, c_R, ft	1·1	1·7	1·5	1·5
Effectiveness, n_ζ ..	0·035	0·030	0·035	0·07
b_1	−0·18	−0·18	−0·15	0
b_2	−0·20	−0·20	−0·08	−0·07
b_3	—	—	−0·07	−0·07
Inertia, i_R	0·13	0·15	0·2	0·2
Mass moment, m_R, x_R ..	0	+0·07	0	0
m_R	0·15	0·654	1·00	2·00
Tab				
Area, S_T, ft²	—	—	0·8	0·8
Chord, c_T, ft	—	—	0·4	0·4
c_1	—	—	0	+0·10
c_2	—	—	−0·20	−0·10
c_3	—	—	−0·30	−0·30
Inertia, i_T	—	—	0·25	0·25
Mass moment, m_T, x_T ..	—	—	0	−0·07
Tab arm from rudder hinge, l_T, ft	—	—	1·4	1·4
Basic Aircraft				
a_1 fin	1·40	1·25	1·5	1·5
n_r	0·065	0·08	0·08	0·08
T_ψ, V_i, ft..	350	900	1,000	1,000
i_c	0·09	0·12	0·14	0·14

APPENDIX A

Method of Analysis

The aircraft motion considered will be directional snaking ($\psi \equiv -\beta$) with rudder freedom, ζ, and tab freedom, ζ_T, if required. The neglected freedoms, rolling and sideways movement of the c.g. will of course affect the stability of the actual motion of the aircraft but the contribution of the rudder will be basically the same in either case.

In consequence of the above assumptions only yawing moments N, rudder hinge moments H and tab hinge moments H_T will be considered. Thus the equations of motion to be dealt with are

$$\tfrac{1}{2}\rho V^2 Sb\left(n_\psi \psi + n_r \frac{\dot{\psi} b}{2V} + n_\zeta \zeta\right) = C\ddot{\psi} \quad \text{(A.1)}$$

$$\tfrac{1}{2}\rho V^2 S_R c_R (b_1\psi + b_2\zeta + b_3\zeta_T) + \frac{\partial H}{\partial \dot{\zeta}}\dot{\zeta} = \theta(\ddot{\zeta} + \ddot{\psi}) - m_R x_R l_F \ddot{\psi} \quad \text{(A.2)}$$

$$\tfrac{1}{2}\rho V^2 S_T c_T (c_1\psi + c_2\zeta + c_3\zeta_T) + \frac{\partial H}{\partial \dot{\zeta}_T}\dot{\zeta}_T = \theta_T(\ddot{\zeta}_T + \ddot{\zeta} + \ddot{\psi}) - m_T x_T (l_F + l_T)\ddot{\psi} - m_T x_T l_T \ddot{\zeta}. \quad \text{(A.3)}$$

Analysis will be made with the aid of vector methods. The solution will be obtained in two steps :

(i) Finding the response of the free rudder (with or without tab) to the directional oscillation of the aircraft (*see* Appendices B and C).

(ii) Analysing the effect of this rudder motion upon the stability of the aircraft motion.

The method is essentially an iterative procedure but for the majority of cases the first step will give satisfactory results.

The proposed procedure will best be understood by an illustrative example as sketched in Fig. 15, showing the time history of an aircraft harmonically oscillating in yaw with an assumed harmonic rudder motion. The rudder motion, ζ, and correspondingly the associated yawing moment exerted upon the aircraft by the rudder ($N_\zeta \zeta$) can be split up into a component in phase with the aircraft yawing, ψ, and one in phase with the rate of yaw of the aircraft motion, $\dot{\psi}$. The component in phase with ψ ($N_\zeta\, \zeta_\psi$), will contribute to the weathercock-stability of the aircraft.

$$\Delta n_\psi = -\Delta n_v = n_\zeta\left(\frac{\zeta_\psi}{\psi}\right). \quad \text{(A.4)}$$

Similarly the component in phase with $\dot{\psi}$,($N_\zeta \zeta_{\dot{\psi}}$) can be expressed as an additional damping in yaw derivative

$$\Delta n_r = \Delta \frac{\partial C_N}{\partial \dfrac{\dot{\psi} b}{2V}} = n_\zeta\left(\frac{\zeta_{\dot{\psi}}}{\dot{\psi}}\right)\frac{2V}{b}. \quad \text{(A.5)}$$

The rate of yaw amplitude is related to the yaw amplitude by

$$\dot{\psi} = \frac{\psi\omega}{\cos \varepsilon_D} \quad \text{(A.6)}$$

where $\omega = 2\pi/T_\psi$ the angular frequency, and $\varepsilon_D = \tan^{-1}\delta/2\pi$, the damping angle of the oscillation. Thus equation (A.5) may be written :

$$\Delta n_r = n_\zeta\left(\frac{\zeta_{\dot{\psi}}}{\psi}\right)\frac{T_\psi}{2\pi}\frac{2V}{b}\cos \varepsilon_D. \quad \text{(A.7)}$$

The time history of the oscillatory motion in Fig. 15 is more conveniently represented by vectors in the complex plane which must be thought of as rotating with the angular frequency ω of the aircraft motion. The phase relationship between vectors representing derivatives of any variable α of an oscillating system is generally,

$$\varepsilon\left(\frac{d^n\alpha}{dt^n}\right) - \varepsilon\left(\frac{d^m\alpha}{dt^m}\right) = \left(n - m\right)\left(\frac{\pi}{2} + \varepsilon_D\right) \quad \ldots \quad \ldots \quad \ldots \quad \text{(A.8)}$$

and the magnitude relationship is

$$\left|\frac{d^n\alpha}{dt^n}\right| = \left|\frac{d^m\alpha}{dt^m}\right|\left(\frac{\omega}{\cos\,\varepsilon_D}\right)^{(n-m)} \quad \ldots \quad \ldots \quad \ldots \quad \ldots \quad \ldots \quad \ldots \quad \ldots \quad \text{(A.9)}$$

If the vector representing ψ is made the reference of the phase-scale, the variables represented in Fig. 15 will give the vector diagram Fig. 16. ζ and the corresponding yawing moment ($N_\zeta\,\zeta$) can be split up geometrically into components which can be used for the determination of Δn_v and Δn_r in equations A.4 and A.7.

APPENDIX B

Rudder Response

For the rudder response calculations equation A.2 will be re-arranged:

$$\tfrac{1}{2}\rho V^2 S_R c_R b_2 \zeta + \frac{\partial H}{\partial \dot{\zeta}}\,\dot{\zeta} - \theta\ddot{\zeta} = -\,\tfrac{1}{2}\rho V^2 S_R c_R b_1 \psi + (\theta - m_R x_R l_F)\ddot{\psi}. \quad \ldots \quad \text{(B.1)}$$

The aircraft motion $\psi(t)$ will be considered as the forcing function and will generally be a damped oscillation

$$\psi(t) = \psi_0\, e^{(\lambda + i\omega)t}.$$

Apart from a transient state, which will be neglected here, the rudder will respond correspondingly

$$\zeta(t) = \zeta_0\, e^{(\lambda + i\omega)t}.$$

Substituting these expressions and their derivatives in equation B.1 an algebraic expression for the frequency response of the rudder is obtained:

$$\frac{\zeta_0}{\psi_0} = -\,\frac{b_1}{b_2}\,\frac{1 + \dfrac{\sigma_\theta - \sigma_M}{b_1}\left\{1 - i\left(\dfrac{\lambda}{\omega}\right)2 - \left(\dfrac{\lambda}{\omega}\right)^2\right\}}{1 + \left(\dfrac{\partial H}{\partial \dot{\zeta}}\right)\dfrac{\omega}{H_\zeta}\left(\dfrac{\lambda}{\omega} + i\right) + \dfrac{\sigma_\theta}{b_2}\left\{1 - i\,\dfrac{\lambda}{\omega}\,2 - \left(\dfrac{\lambda}{\omega}\right)^2\right\}}. \quad \ldots \quad \text{(B.2)}$$

This is a complex expression, the real part of which gives the rudder amplitude in phase with ψ and the imaginary part the rudder amplitude 90 deg phase leading against ψ.

$\lambda/\omega = -\tan\varepsilon_D = -\,\delta/2\pi$ is the damping of the aircraft oscillation and ω its angular frequency. σ_θ and σ_M represent rudder inertia and mass as defined in equation (8) and (9). H_ζ is the rudder restoring derivative ($b_2\tfrac{1}{2}\rho V^2 S_R\, c_R$) in lb ft/radn.

Solving equation B.2 gives a vector for the rudder motion ζ with respect to ψ; this vector can be split up into its components in phase with ψ and with $\dot{\psi}$, as explained in Appendix A, and in Fig. 16, and used with equations A.4 and A.7 for the determination of Δn_v and Δn_r.

If the aircraft motion is only moderately damped (or undamped), say for logarithmic decrements $|\delta| < 2 \cdot 0$ the term λ/ω can be neglected. This simplifies equation B.2 and approximations for the real and imaginary part are obtained :

$$\left|\frac{\zeta_0}{\psi_0}\right|_{\mathrm{Re}} \doteq -\frac{b_1}{b_2} \frac{1 + \dfrac{\sigma_0 - \sigma_M}{b_1}}{1 + \dfrac{\sigma_0}{b_2}} \frac{1}{1 + D^2} \quad \ldots \quad \text{(B.3)}$$

$$\left|\frac{\zeta_0}{\psi_0}\right|_{\mathrm{Im}} \doteq \frac{b_1}{b_2} \frac{1 + \dfrac{\sigma_0 - \sigma_M}{b_1}}{1 + \dfrac{\sigma_0}{b_2}} \frac{D}{1 + D^2} \quad \ldots \quad \text{(B.4)}$$

where D represents rudder damping :

$$D = \frac{\partial H}{\partial \xi} \frac{\omega}{H_\zeta} \frac{1}{1 + \dfrac{\sigma_0}{b_2}} \quad \ldots \quad \text{(B.5)}$$

The effect of the rudder motion on the damping of the aircraft will be a maximum if the rudder component in phase with $\dot{\psi}$ is a maximum, *i.e.*, if $(\zeta_0/\psi_0)_{\mathrm{Im}} = \max$ or $d\{(\zeta_0/\psi_0)_{\mathrm{Im}}\}/dD = 0$. This gives as the condition for optimum rudder damping, $D = 1$, or

$$\frac{\partial H}{\partial \xi} = V_i \frac{T_\psi V_i}{2\pi} \left(1 + \frac{\sigma_0}{b_2}\right) \frac{\rho_0}{2} S_R c_R b_2. \quad \ldots \quad \text{(B.6)}$$

$(T_\psi V_i)$, the wavelength of the lateral oscillation, can practically be regarded as constant over the speed range. Thus rudder damping should vary linearly with V_i—and with b_2, if this derivative changes—in order to have optimum aircraft damping throughout the speed range. If a mechanical damper is used, it will have to be adjusted to give optimum operation at one speed V_{SET} and the rudder damping parameter D varies then over the speed range as $D = V_{\mathrm{SET}}/V_i$, if $b_2 = \text{const.}$ Substituting this expression for D in equations B.3 and B.4 and using equations A.4 and A.7 approximations are obtained for

$$\Delta n_v = n_\zeta \frac{b_1}{b_2} \frac{1 + \dfrac{\sigma_0 - \sigma_M}{b_1}}{1 + \dfrac{\sigma_0}{b_2}} \frac{1}{1 + (V_{\mathrm{SET}}/V_i)^2} \quad \ldots \quad \text{(B.7)}$$

$$\Delta n_r = n_\zeta \frac{b_1}{b_2} \frac{T_\psi V_i}{\pi b} \sqrt{\left(\frac{\rho_0}{\rho}\right)} \frac{1 + \dfrac{\sigma_0 - \sigma_M}{b_1}}{1 + \dfrac{\sigma_0}{b_2}} \frac{V_{\mathrm{SET}}/V_i}{1 + (V_{\mathrm{SET}}/V_i)^2} \quad \ldots \quad \text{(B.8)}$$

The response function expressed by equation B.2 may be plotted graphically against the various parameters involved and the rudder response vector (ζ_0/ψ_0) can then be read from such a diagram and split up into its components in phase with ψ and with $\dot{\psi}$ as illustrated in Fig. 18.

These components will then be substituted into equations A.4 and A.7 respectively to obtain Δn_v and Δn_r.

For such a graphical presentation the number of parameters has to be reduced and it is proposed to neglect λ/ω in the numerator of equation B.2, which will now read :

$$\frac{\zeta_0}{\psi_0} = \frac{-\frac{b_1}{b_2}\left(1 + \frac{\sigma_\theta - \sigma_M}{b_1}\right)}{1 + \frac{\partial H}{\partial \zeta}\frac{\omega}{H_\zeta}\left(\frac{\lambda}{\omega} + i\right) + \frac{\sigma_\theta}{b_2}\left\{1 - i\frac{\gamma}{\omega}2 - \left(\frac{\lambda}{\omega}\right)^2\right\}}$$

or

$$\frac{\zeta_0/\psi_0}{\frac{b_1}{b_2}\left(1 + \frac{\sigma_\theta - \sigma_M}{b_1}\right)} = \frac{-1}{1 + \frac{\partial H}{\partial \zeta}\frac{\omega}{H\zeta}\left(\frac{\lambda}{\omega} + i\right) + \frac{\sigma_\theta}{b_2}\left\{1 - i\frac{\lambda}{\omega}2 - \left(\frac{\lambda}{\omega}\right)^2\right\}} = R . \qquad \text{(B.9)}$$

Vector graphs representing the response function R for values of aircraft damping $\delta = 2\pi\lambda/\omega$ of $-1 \cdot 0$, 0, $1 \cdot 0$, $2 \cdot 0$, $3 \cdot 0$ and $4 \cdot 0$ are plotted in Figs. 19 to 24. Aircraft rate of yaw, $\dot{\psi}$, is represented in these graphs by a vector leading in phase by (90 deg + ε_D) against ψ. Thus the component of R in phase with $\dot{\psi}$ has to be read under this angle as illustrated in Fig. 17, where a positive damping angle ε_D is assumed.

In equation A.7 the rudder vector is used in the form ($\zeta_{\dot{\psi}}/\psi \cos \varepsilon_D$) ; consequently the scales for the $\dot{\psi}$ component of R are given in that form.

For computing with the aid of response function R, equations A.4 and A.7 are rewritten as :

$$\Delta n_v = n_\zeta \frac{b_1}{b_2}\left(1 + \frac{\sigma_\theta - \sigma_M}{b_1}\right) R_\psi \qquad \text{(B.10)}$$

$$\Delta n_r = - n_\zeta \frac{b_1}{b_2}\left(1 + \frac{\sigma_\theta - \sigma_M}{b_1}\right) R_{\dot{\psi}} \frac{T_\psi}{2\pi}\frac{2V}{b} \cos \varepsilon_D . \qquad \text{(B.11)}$$

APPENDIX C

Rudder-Tab-Response

For the determination of the motion of a rudder with a freely hinged tab attached to it, equations A.2 and A.3 will be considered. The equation of rudder hinge moments will be simplified by assuming the rudder to be aerodynamically neutral ($b_1 = 0$) and to have no mass and inertia. Thus,

$$\tfrac{1}{2}\rho V^2 S_R c_R (b_2 \zeta + b_3 \zeta_T) + \frac{\partial H}{\partial \dot{\zeta}} \dot{\zeta} = 0 \qquad \text{(C.1)}$$

$$\tfrac{1}{2}\rho V^2 S_T c_T (c_2 \zeta + c_3 \zeta_T) + \frac{\partial H_T}{\partial \dot{\zeta}_T} \dot{\zeta}_T - \theta_T(\ddot{\zeta} + \ddot{\zeta}_T) + m_T x_T l_T \ddot{\zeta} =$$
$$- \tfrac{1}{2}\rho V^2 S_T c_T\, c_1 \psi + (\theta_T - m_T x_T l_F)\ddot{\psi} . \qquad \text{(C.2)}$$

Substituting

$$\zeta = \zeta_0\, e^{(\lambda + i\omega)t} ; \quad \psi = \psi_0\, e^{(\lambda + i\omega)t} ; \quad \zeta_T = \zeta_{T0}\, e^{(\lambda + i\omega)t}$$

the response of the rudder ζ_0 to the aircraft motion ψ_0 is obtained as

$$\frac{\zeta_0}{\psi_0}=\frac{c_1 b_3}{c_3 b_2}\,\frac{1+\frac{\tau_\beta}{c_1}\left[1-\left(\frac{\lambda}{\omega}\right)^2\right]-i2\frac{\lambda}{\omega}\frac{\tau_\beta}{c_1}}{\left[\begin{array}{l}1-\frac{c_2 b_3}{c_3 b_2}+(D_R+D_T)\left(\frac{\lambda}{\omega}\right)-\left(D_R D_T+\frac{\tau_\zeta b_3}{c_3 b_2}\right)\left[1-\left(\frac{\lambda}{\omega}\right)^2\right]+\frac{\tau_T}{c_3}D_R\left[\left(\frac{\lambda}{\omega}\right)^3-3\frac{\lambda}{\omega}\right]\\ \quad+i\left\{D_R+D_T+\left(D_R D_T+\frac{\tau_\zeta}{c_3}\frac{b_3}{b_2}\right)2\frac{\lambda}{\omega}+\frac{\tau_{\theta T}}{c_3}D_R\left[1-3\left(\frac{\lambda}{\omega}\right)^2\right]\right\}\end{array}\right]}. \quad \text{(C.3)}$$

The tab parameters τ_β, τ_ζ and $\tau_{\theta T}$ are defined in equation 15. D_R and D_T represent rudder and tab damping

$$D_R=\frac{\partial H}{\partial \zeta}\,\frac{2}{b_2}\,\frac{2\pi}{T_\psi V_i}\,\frac{1}{\rho_0 V_i S_R c_R} \quad \text{(C.4)}$$

$$D_T=\frac{\partial H_T}{\partial \zeta_T}\,\frac{2}{c_3}\,\frac{2\pi}{T_\psi V_i}\,\frac{1}{\rho_0 V_i S_T c_T} \quad \text{(C.5)}$$

The response function equation (C.3) can be used to obtain the components of the rudder motion in phase with ψ and with $\dot\psi$ and thus to calculate Δn_v and Δn_r with equations A.4 and A.7.

For moderate aircraft damping $|\,\delta\,| < 2\cdot 0$, λ/ω can be neglected in equation (C.3) and approximations for the real and imaginary part of the solution can be obtained :

$$\left|\frac{\zeta_0}{\psi_0}\right|_{\mathrm{Re}}=+\frac{c_1 b_3}{c_3 b_2}\,\frac{\left\{1-D_R D_T-\frac{b_3}{b_2}\frac{\tau_\zeta+c_2}{c_3}\right\}\left(1+\frac{\tau_\beta}{c_1}\right)}{\left\{1-D_R D_T-\frac{b_3}{b_2}\frac{\tau_\zeta+c_2}{c_3}\right\}^2+\left\{D_T+D_R\left(1+\frac{\tau_{\theta T}}{c_3}\right)\right\}^2} \quad \text{(C.6)}$$

$$\left|\frac{\zeta_0}{\psi_0}\right|_{\mathrm{Im}}=-\frac{c_1 b_3}{c_3 b_2}\,\frac{\left\{D_T+D_R\left(1+\frac{\tau_{\theta T}}{c_3}\right)\right\}\left(1+\frac{\tau_\beta}{c_1}\right)}{\left\{1-D_R D_T-\frac{b_3}{b_2}\frac{\tau_\zeta+c_2}{c_3}\right\}^2+\left\{D_T+D_R\left(1+\frac{\tau_{\theta T}}{c_3}\right)\right\}^2}. \quad \text{(C.7)}$$

Optimum tab damping again is determined by differentiating $d\{(\zeta_0/\psi)_{\mathrm{Im}}\}/dD_T$. This gives

$$\frac{\partial H_T}{\partial \zeta_T}=V_i c_3\left(\frac{T_\psi V_i}{2\pi}\right)\frac{\rho_0}{2}\,\frac{S_T C_T}{1-D_R}\left\{1-\frac{b_3}{b_2}\frac{\tau_\zeta+c_2}{c_3}-D_R\left(1+\frac{\tau_{\theta T}}{c_3}\right)\right\}. \quad \text{(C.8)}$$

If the tab damper is set to give optimum yaw damping at V_{SET}, the effective damping will vary over the speed range according to

$$\frac{D_T+D_R\left(1+\frac{\tau_{\theta T}}{c_3}\right)}{1-\frac{b_3}{b_2}\frac{\tau_\zeta+c_2}{c_3}-D_R D_T}=\frac{V_{\mathrm{SET}}}{V_i}. \quad \text{(C.9)}$$

Using this expression with equations (C.6), (C.7), (A.4) and (A.7) useful approximations for Δn_v and Δn_r are obtained:

$$\Delta n_v = -2\frac{n_\zeta}{c_3}\frac{b_3}{b_2}\frac{m_T}{\rho_0 S_T}\left(\frac{2\pi}{T_\psi V_i}\right)^2\left(i_T c_T - \frac{x_T}{c_T} l_F\right)\frac{1+\dfrac{c_1}{\tau_\beta}}{1+(V_{\text{SET}}/V_i)^2} \times$$

$$\times\left\{1 - \frac{b_3}{b_2}\frac{\tau_\zeta + c_2}{c_3} + D_R\left(D_R - \frac{V_{\text{SET}}}{V_i}\right)\right\}^{-1} \quad \ldots \quad \text{(C.10)}$$

$$\Delta n_r = -4\frac{n_\zeta}{c_3}\frac{b_3}{b_2}\frac{m_T}{\rho_0 S_T}\frac{2\pi}{T_\psi V_i}\sqrt{\left(\frac{\rho_0}{\rho}\right)}\left(i_T c_T - \frac{x_T}{c_T} l_F\right)\left(1+\frac{c_1}{\tau_\beta}\right) \times$$

$$\times\frac{V_{\text{SET}}/V_i}{1+(V_{\text{SET}}/V_i)^2}\left\{1 - \frac{b_3}{b_2}\frac{\tau_\zeta + c_2}{c_3} + D_R\left(D_R - \frac{V_{\text{SET}}}{V_i}\right)\right\}^{-1}. \quad \ldots \quad \text{(C.11)}$$

If more accurate expressions for Δn_v and Δn_r are required than those given by equations (C.10) and (C.11), equation (C.3) has to be solved for each individual case.

List of Symbols used in the Appendices

D		Rudder damping parameter (equation (B.5))
D_R		Rudder damping parameter (equation (C.4))
D_T		Tab damping parameter (equation (C.5))
i	=	$\sqrt{-1}$, Imaginary number
R		Rudder response function
R_ψ		Rudder response vector in phase with ψ
$R_{\dot\psi}$		,, ,, ,, ,, ,, ,, $\dot\psi$
δ		Log. decrement of the lateral oscillation
λ		Damping ,, ,, ,, ,,
ω		Frequency ,, ,, ,, ,,
ω_R		Natural frequency of the rudder
ζ_ψ		Rudder vector in phase with ψ
$\zeta_{\dot\psi}$		,, ,, ,, ,, ,, $\dot\psi$

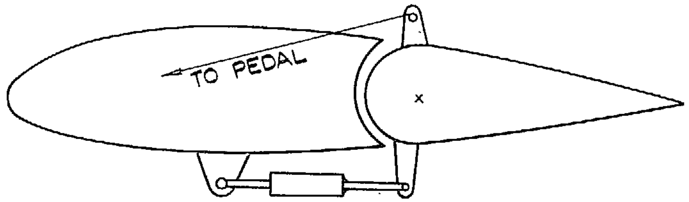

FIG. 1. Main control surface restrained by damper

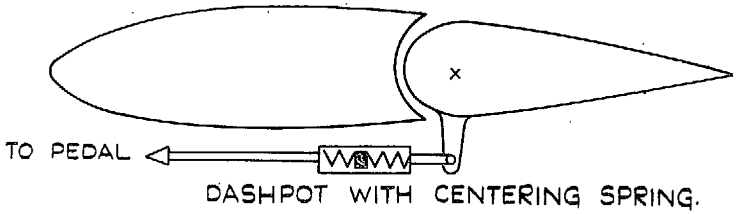

FIG. 2. Damper within the control circuit

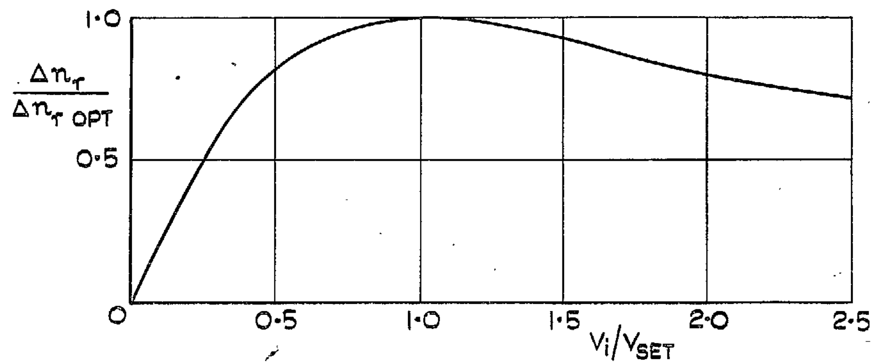

FIG. 3. Variation of damping effectiveness with speed for fixed damper setting.

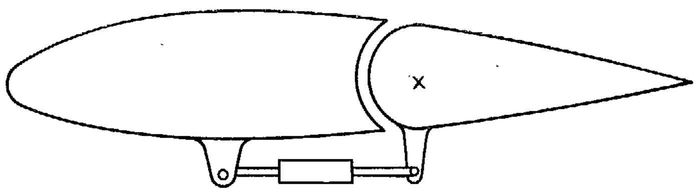

FIG. 4. Additional damping surface.

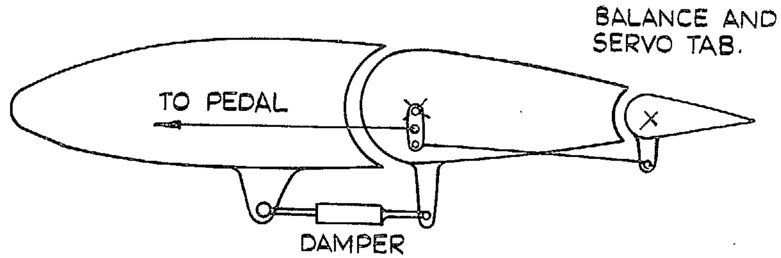

FIG. 5. Servo-tab controlled separate damping surface.

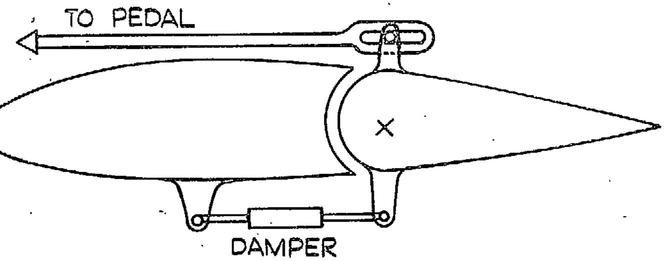

FIG. 6. Damping surface connected with backlash to the control circuit.

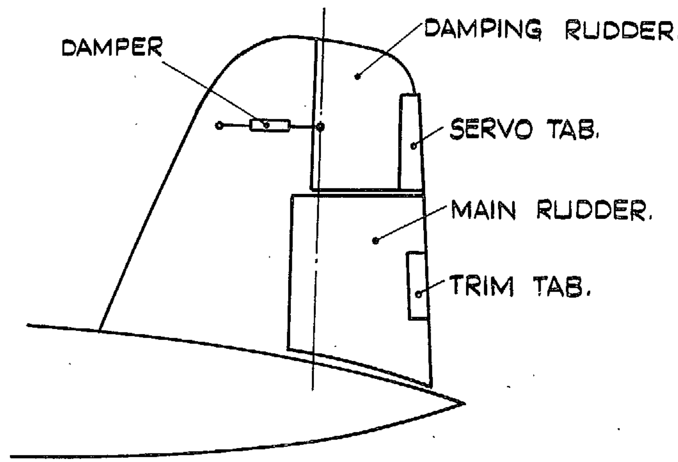

FIG. 7. Servo-tab controlled additional damping rudder.

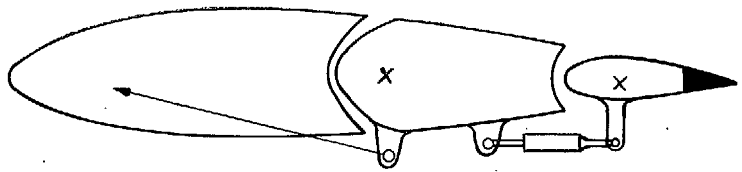

FIG. 8. Damping tab hinged to main control surface.

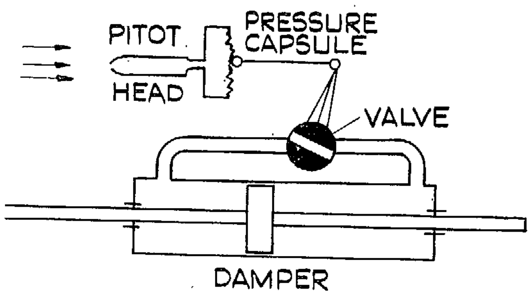

FIG. 9. Hydraulic dashpot with V_i-controlled by-pass.

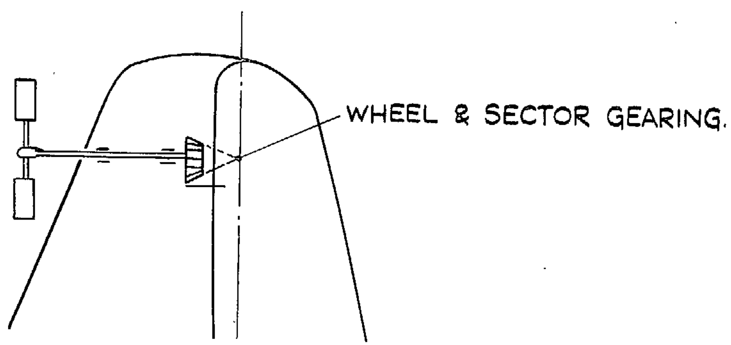

FIG. 10. Aerodynamic paddle damper.

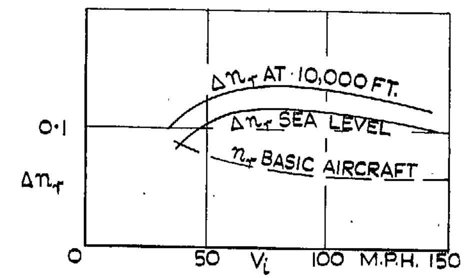

FIG. 11. Gain in aircraft damping from damped main rudder (example A).

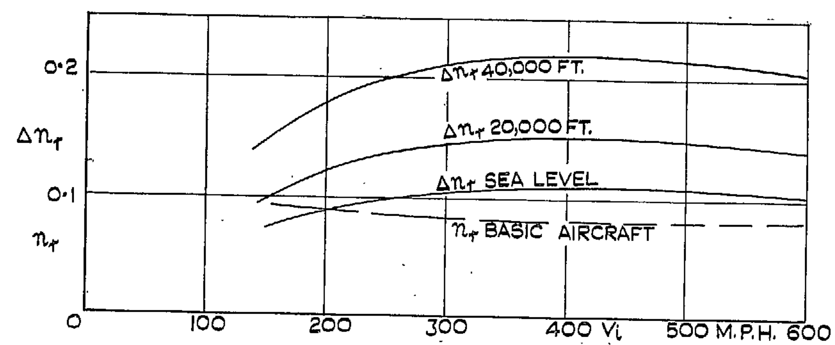

FIG. 12. Gain in aircraft damping from one damping rudder of a twin-fin fighter (example B).

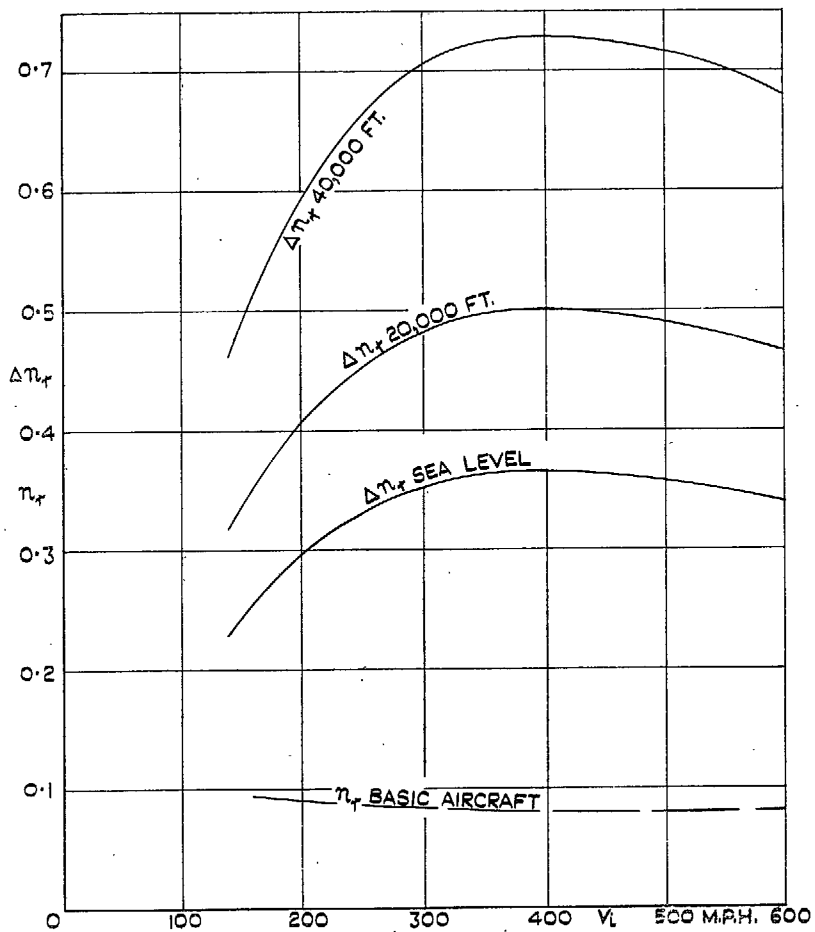

FIG. 13. Gain in aircraft damping from separate damping rudder with balance tab (example C).

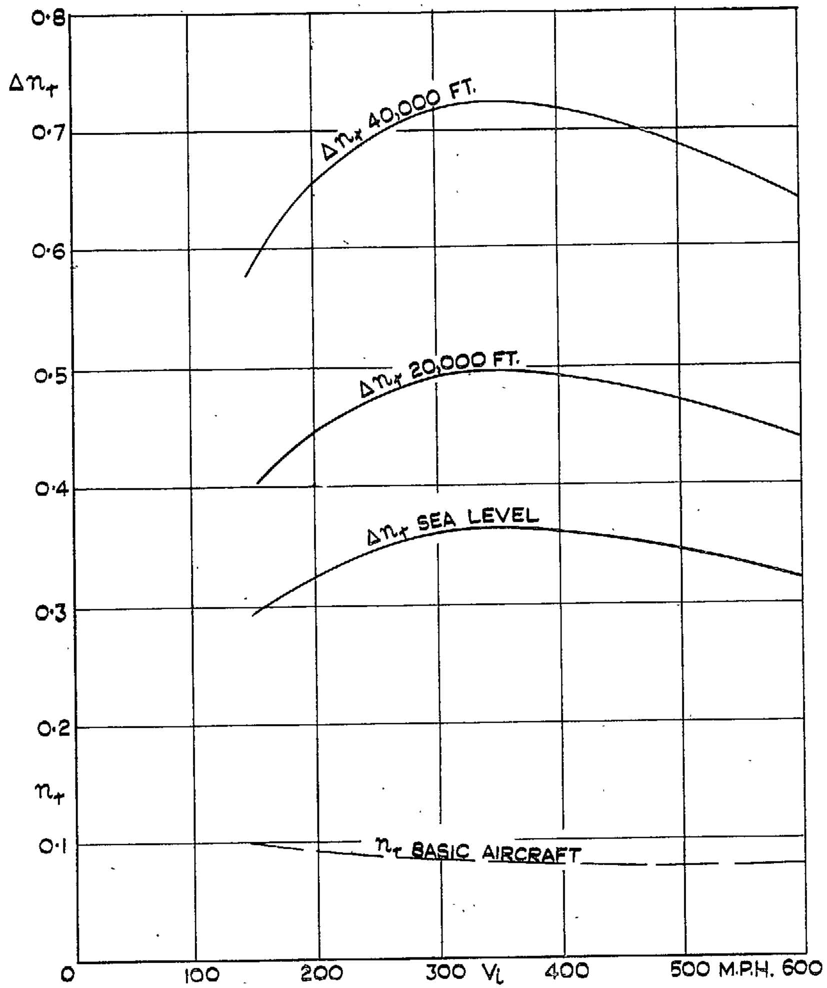

FIG. 14. Gain in aircraft damping from damping tab (example D).

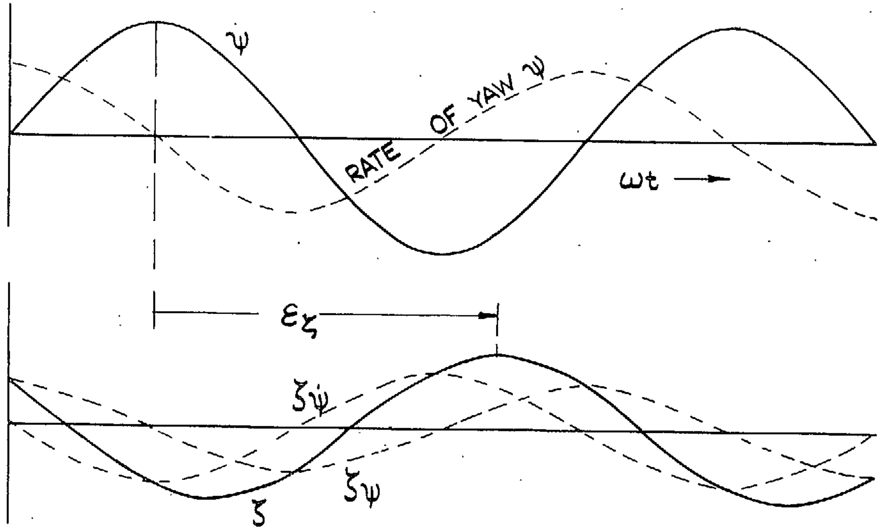

FIG. 15. Time history of the harmonic lateral oscillation of an aircraft with free rudder.

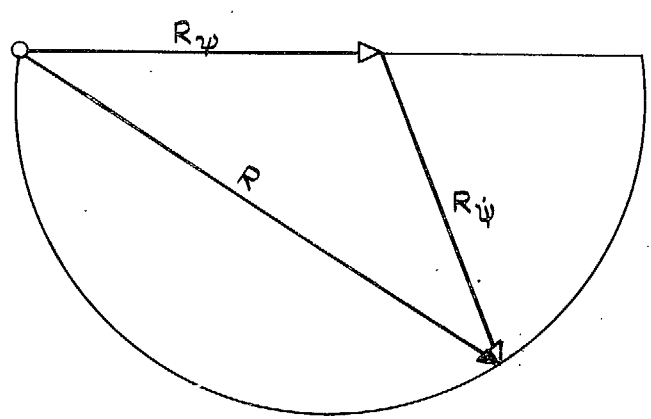

FIG. 17. Evaluation of the components in phase with ψ and $\dot{\psi}$ of the rudder response vector (R).

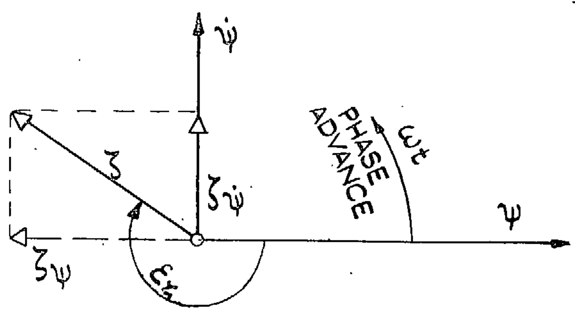

FIG. 16. Vector representation of the variables of the aircraft motion illustrated in fig. 15.

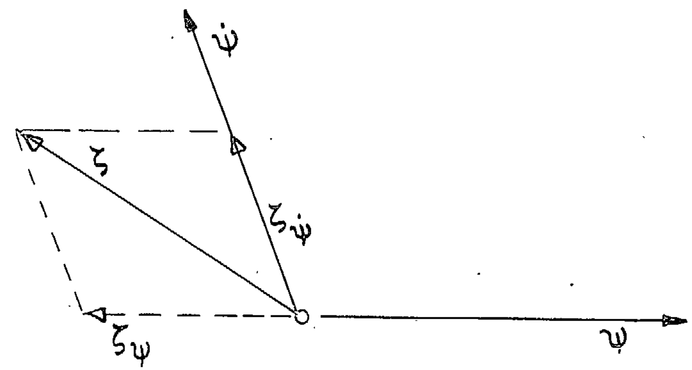

FIG. 18. Vector diagram of the rudder motion against aircraft motion corresponding to the case illustrated in fig. 17 (assuming $b_1 < 0$).

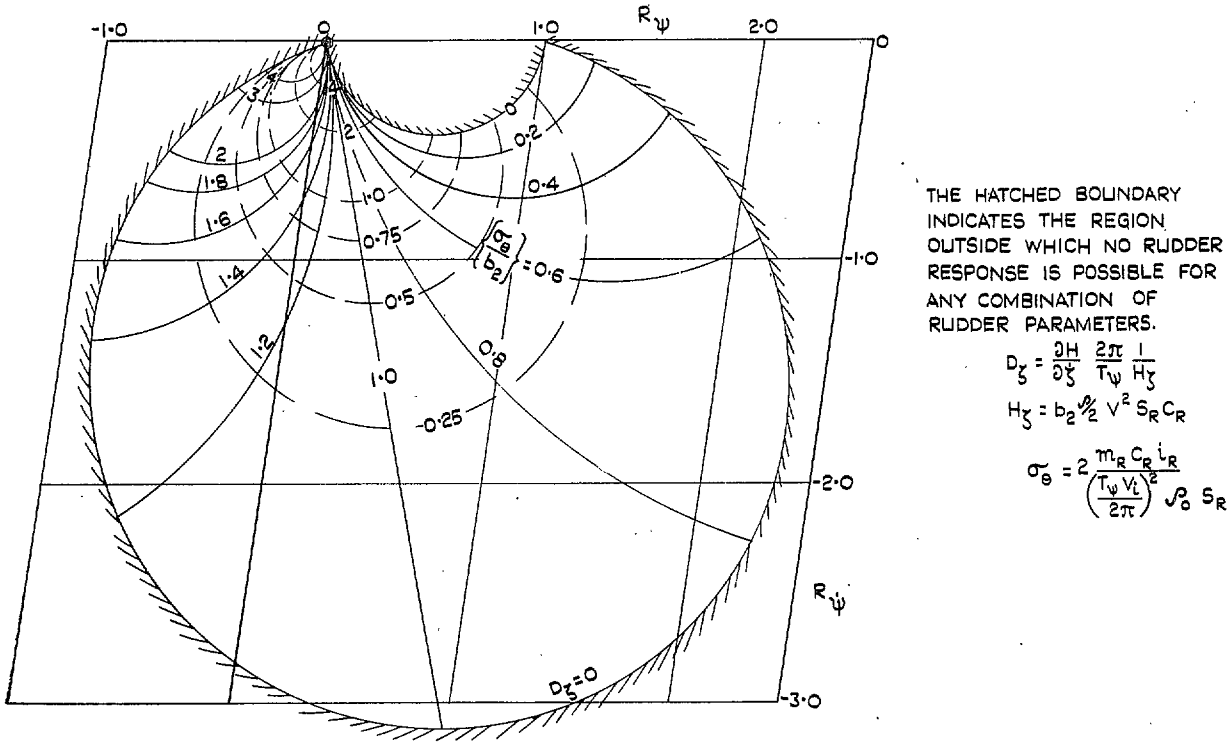

FIG. 19. Rudder response diagram for aircraft damping $\delta = -1 \cdot 0$.

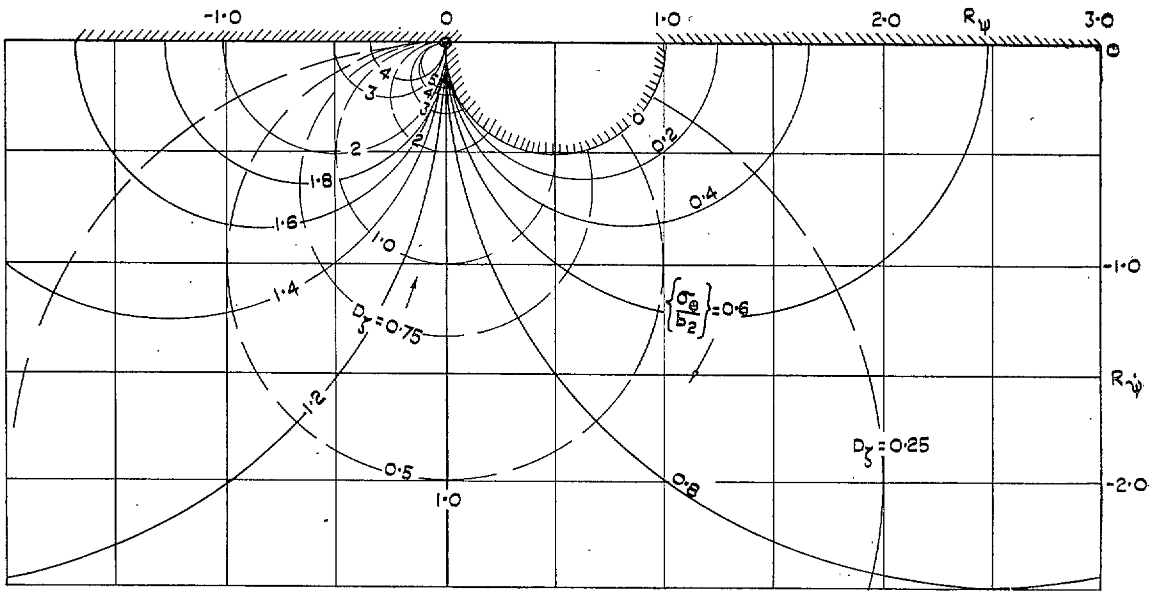

FIG. 20. Rudder response diagram for undamped aircraft motion. $\delta = 0$.

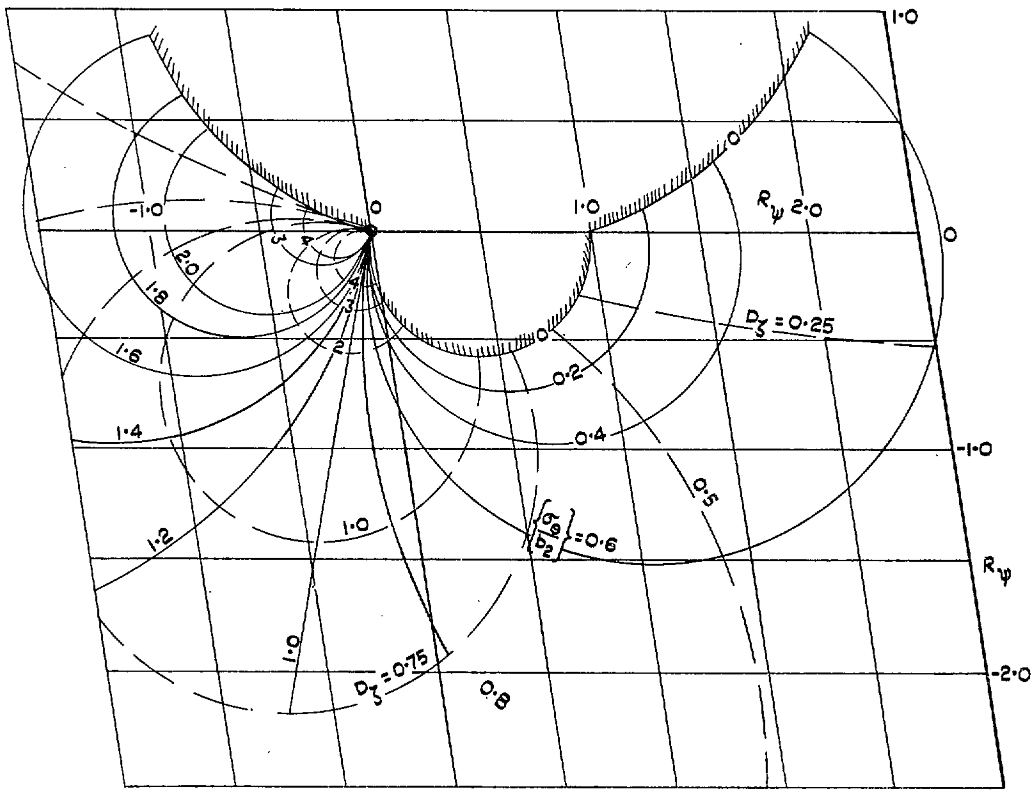

FIG. 21. Rudder response diagram for aircraft damping. $\delta = 1 \cdot 0$.

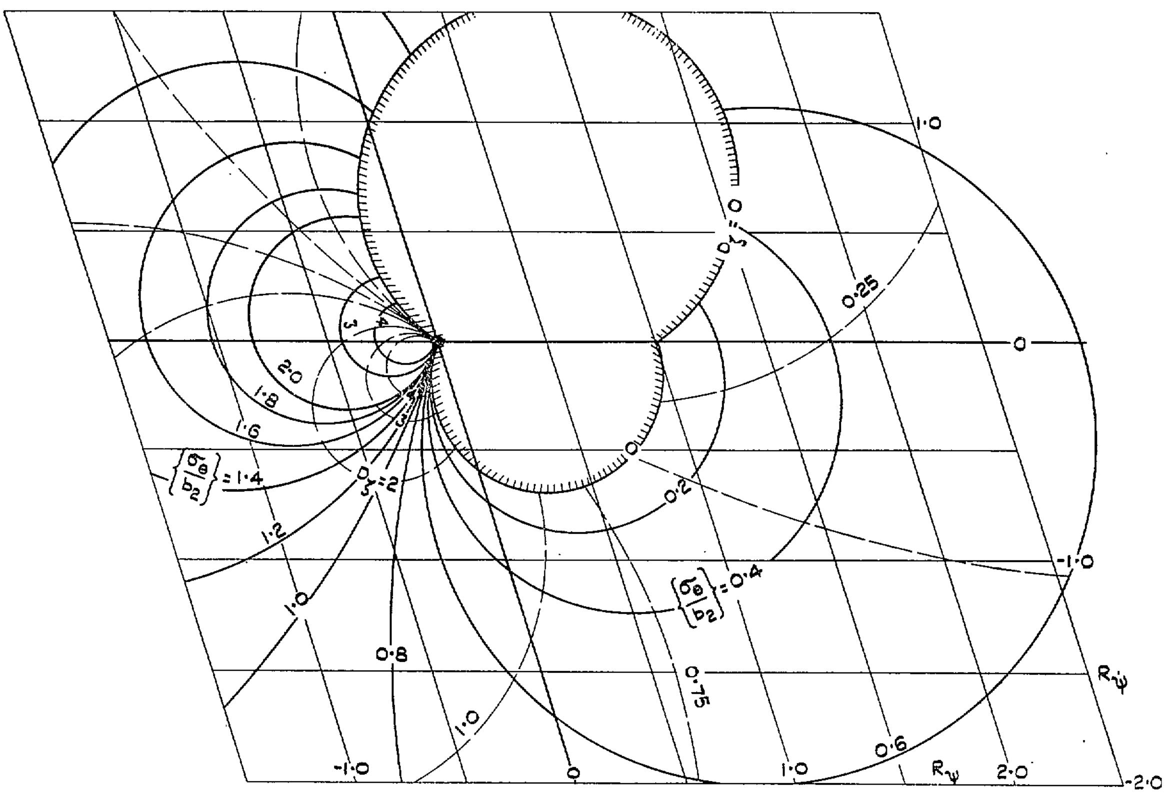

FIG. 22. Rudder response diagram for aircraft damping. $\delta = 2 \cdot 0$.

C

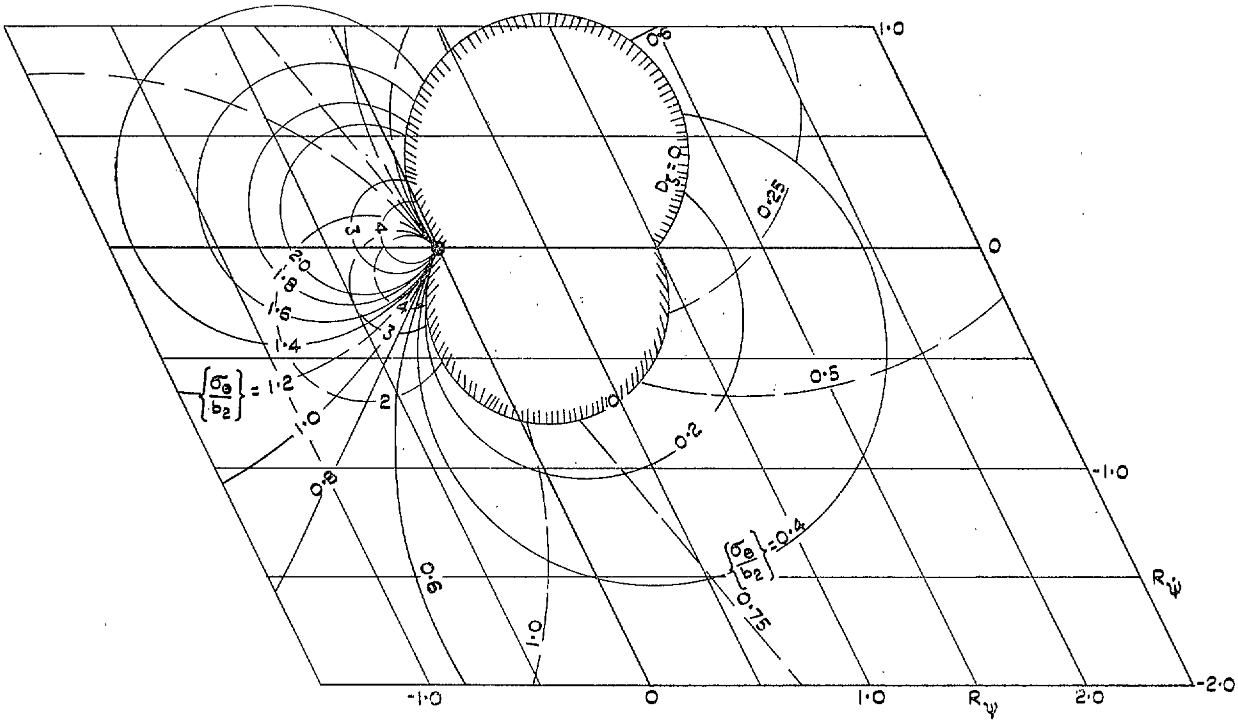

FIG. 23. Rudder response diagram for aircraft damping. $\delta = 3 \cdot 0$.

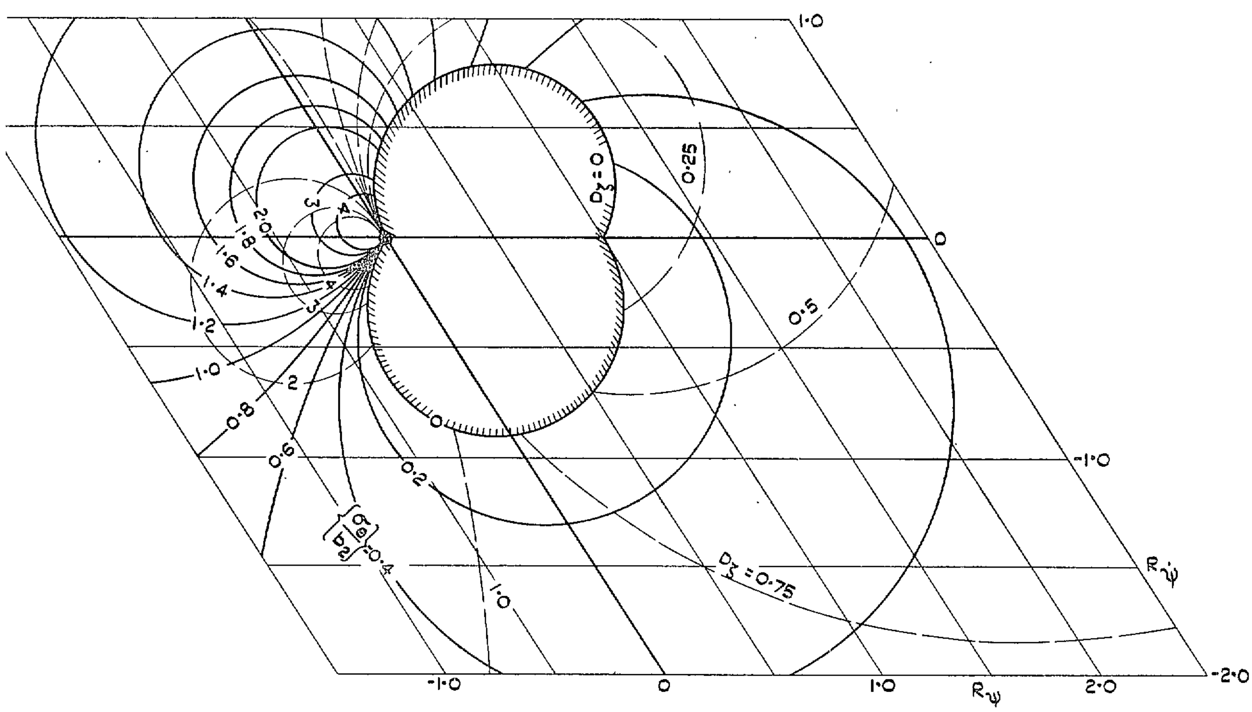

FIG. 24. Rudder response diagram for aircraft damping. $\delta = 4 \cdot 0$.

Publications of the Aeronautical Research Council

ANNUAL TECHNICAL REPORTS OF THE AERONAUTICAL RESEARCH COUNCIL (BOUND VOLUMES)

1939 Vol. I. Aerodynamics General, Performance, Airscrews, Engines. 50s. (51s. 9d.)
Vol. II. Stability and Control, Flutter and Vibration, Instruments, Structures, Seaplanes, etc. 63s. (64s. 9d.)

1940 Aero and Hydrodynamics, Aerofoils, Airscrews, Engines, Flutter, Icing, Stability and Control, Structures, and a miscellaneous section. 50s. (51s. 9d.)

1941 Aero and Hydrodynamics, Aerofoils, Airscrews, Engines, Flutter, Stability and Control, Structures. 63s. (64s. 9d.)

1942 Vol. I. Aero and Hydrodynamics, Aerofoils, Airscrews, Engines. 75s. (76s. 9d.)
Vol. II. Noise, Parachutes, Stability and Control, Structures, Vibration, Wind Tunnels. 47s. 6d. (49s. 3d.)

1943 Vol. I. Aerodynamics, Aerofoils, Airscrews. 80s. (81s. 9d.)
Vol. II. Engines, Flutter, Materials, Parachutes, Performance, Stability and Control, Structures. 90s. (92s. 6d.)

1944 Vol. I. Aero and Hydrodynamics, Aerofoils, Aircraft, Airscrews, Controls. 84s. (86s. 3d.)
Vol. II. Flutter and Vibration, Materials, Miscellaneous, Navigation, Parachutes, Performance, Plates and Panels, Stability, Structures, Test Equipment, Wind Tunnels. 84s. (86s. 3d.)

1945 Vol. I. Aero and Hydrodynamics, Aerofoils. 130s. (132s. 6d.)
Vol. II. Aircraft, Airscrews, Controls. 130s. (132s. 6d.)
Vol. III. Flutter and Vibration, Instruments, Miscellaneous, Parachutes, Plates and Panels, Propulsion. 130s (132s. 3d.)
Vol. IV. Stability, Structures, Wind tunnels, Wind Tunnel Technique. 130s. (132s. 3d.)

ANNUAL REPORTS OF THE AERONAUTICAL RESEARCH COUNCIL—

1937 2s. (2s. 2d.)   1938 1s. 6d. (1s. 8d.)   1939–48 3s. (3s. 3d.)

INDEX TO ALL REPORTS AND MEMORANDA PUBLISHED IN THE ANNUAL TECHNICAL REPORTS, AND SEPARATELY—

April, 1950 - - - - - R. & M. No. 2600. 2s. 6d. (2s. 8d.)

AUTHOR INDEX TO ALL REPORTS AND MEMORANDA OF THE AERONAUTICAL RESEARCH COUNCIL—

1909–January, 1954 - - - - R. & M. No. 2570. 15s. (15s. 6d.)

INDEXES TO THE TECHNICAL REPORTS OF THE AERONAUTICAL RESEARCH COUNCIL—

December 1, 1936 — June 30, 1939.	R. & M. No. 1850.	1s. 3d. (1s. 5d.)
July 1, 1939 — June 30, 1945. -	R. & M. No. 1950.	1s. (1s. 2d.)
July 1, 1945 — June 30, 1946. -	R. & M. No. 2050.	1s. (1s. 2d.)
July 1, 1946 — December 31, 1946.	R. & M. No. 2150.	1s. 3d. (1s. 5d.)
January 1, 1947 — June 30, 1947. -	R. & M. No. 2250.	1s. 3d. (1s. 5d.)

PUBLISHED REPORTS AND MEMORANDA OF THE AERONAUTICAL RESEARCH COUNCIL—

Between Nos. 2251–2349. - -	R. & M. No. 2350.	1s. 9d. (1s. 11d.)
Between Nos. 2351–2449. - -	R. & M. No. 2450.	2s. (2s. 2d.)
Between Nos. 2451–2549. - -	R. & M. No. 2550.	2s. 6d. (2s. 8d.)
Between Nos. 2551–2649. - -	R. & M. No. 2650.	2s. 6d. (2s. 8d.)

Prices in brackets include postage

HER MAJESTY'S STATIONERY OFFICE

York House, Kingsway, London W.C.2; 423 Oxford Street, London W.1; 13a Castle Street, Edinburgh 2; 39 King Street, Manchester 2; 2 Edmund Street, Birmingham 3; 109 St. Mary Street, Cardiff; Tower Lane, Bristol 1; 80 Chichester Street, Belfast, *or through any bookseller*

S.O. Code No. 23-2962

R. & M. No. 2962